JACS JOURNAL OF THE AMERICAN CHEMICAL SOCIETY

Article

pubs.acs.org/JACS

$Pb_2Ba_3(BO_3)_3Cl$: A Material with Large SHG Enhancement Activated by Pb-Chelated BO_3 Groups

Xiaoyu Dong,[†,‡,#] Qun Jing,[†,#] Yunjing Shi,[†,‡] Zhihua Yang,*[,†] Shilie Pan,*[,†] Kenneth R. Poeppelmeier,[§] Joshua Young,[∥] and James M. Rondinelli*[,⊥]

[†]Key Laboratory of Functional Materials and Devices for Special Environments of CAS, Xinjiang Technical Institute of Physics & Chemistry of CAS, Xinjiang Key Laboratory of Electronic Information Materials and Devices, 40-1 South Beijing Road, Urumqi 830011, China

[‡]Engineering Department of Chemistry and Environment, Xinjiang Institute of Engineering, 236 Nanchang Road, Urumqi 830091, China

[§]Department of Chemistry, Northwestern University, 2145 Sheridan Road, Evanston, Illinois 60208-3113, United States

[∥]Department of Materials Science and Engineering, Drexel University, 3141 Chestnut Street, Philadelphia, Pennsylvania 19104-2816, United States

[⊥]Department of Materials Science and Engineering, Northwestern University, 2220 Campus Drive, Evanston, Illinois 60208-0893, United States

Supporting Information

ABSTRACT: Pb(II) has long been associated with lone pair activity and is often substituted in alkali earth metal borates to create new nonlinear optical (NLO) materials with enhanced second harmonic generation (SHG) capabilities. However, large enhancement in isomorphic Pb-free analogues is rare. Here we report a new NLO material $Pb_2Ba_3(BO_3)_3Cl$ with a phase-matching SHG response approximately 3.2× that of KDP and 6× higher than its isomorphic compound $Ba_5(BO_3)_3Cl$. We show that the enhanced SHG response originates from a unique edge-sharing connection between lead–oxygen polyhedra and boron–oxygen groups, making the dielectric susceptibility more easily affected by the external electric field of an incident photon. This understanding provides a route to identify systems that would benefit from SHG-active cation substitution in isomorphic structures that exhibit weak or null SHG responses.

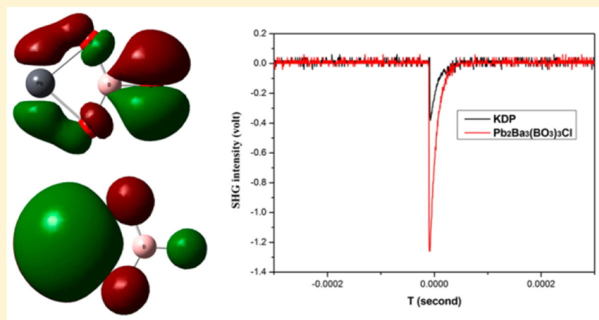

Over the past few decades, nonlinear optical (NLO) materials have attracted considerable attention as key materials to produce coherent light via frequency conversion in solid state lasers,[1−4] with uses extending from the ultraviolet[5−7] to infrared regions.[8−10] A variety of commercial NLO crystals have been developed, including β-BaB_2O_4 (BBO),[11] LiB_3O_5 (LBO),[12] CsB_3O_5 (CBO),[13] $CsLiB_6O_{10}$ (CLBO),[14] $KBe_2BO_3F_2$ (KBBF),[15] $AgGaS_2$,[16−18] and $ZnGeP_2$.[19] One of the most general strategies to design new inorganic NLO materials is to combine diverse types of active building units consisting of typical anionic groups such as boron/carbon–oxygen units,[20−23] polar-chalcogenide units,[24,25] and distorted polyhedra with either d^0 or d^{10} transition metals[26−32] or stereochemically active lone pair (SCALP) cations.[30,31] For example, a large second harmonic generation (SHG) response has been found in $Cd_4BiO(BO_3)_3$ (6 × KDP),[32] which is attributed to the cooperation of the BiO_6 octahedra (from the SCALP effect), the BO_3 groups, and the CdO_n polyhedra.[32]

The lone-pair activity of Pb(II) makes it a promising cation for substitution in alkali-earth metal borates to acquire new NLO materials with enhanced SHG response.[33−39] However, a large increase is often rare, as many materials do not exhibit any enhancement after making a substitution of the alkali-earth metal cations with Pb(II) (so-called A-L replacements) in borates with isomorphic structures. For instance, the SHG response of $Pb_2B_5O_9Cl$ is only 1.1 times larger than that of isomorphic $Ba_2B_5O_9Cl$.[35,36] A similar phenomenon is also found in $Pb_3B_6O_{11}F_2$, with an SHG efficiency ratio of 1.3 when compared to isomorphic $Ba_3B_6O_{11}F_2$. This raises the question of which structures are likely to undergo SHG enhancements after A-L replacement, and why?

To address this question, we first investigated previously reported $Pb_2B_5O_9Cl$ and $Pb_3B_6O_{11}F_2$, which exhibit structures containing lead atoms surrounded by an interconnected boron–oxygen framework. Taking polar $Pb_2B_5O_9Cl$ for example, the basic $[B_5O_9]^{3-}$ building blocks of polar $Pb_2B_5O_9Cl$ consist of three BO_3 groups and two BO_4 tetrahedra, which can

Received: May 25, 2015
Published: July 6, 2015

DOI: 10.1021/jacs.5b05406
J. Am. Chem. Soc. 2015, 137, 9417−9422

be written as 3Δ2T:<2Δ*T*>-<Δ2T> within the modern description of borate groups developed by Burns et al.[40] The BO_3 group's strong Lewis acidity (like isoelectronic BF_3) makes it the *electron acceptor*.

From a molecular point of view, the Pb-BO_3 connections can manifest as either a *closed* or *open* Pb−B−O ring. The consequence of a closed Pb−B−O ring where two oxygen atoms bond to Pb or an open ring where there is a single bonded oxygen atom may be discerned by examining the electron distribution after chemical bond formation. Figure 1 shows the calculated frontier molecular orbital diagrams of $PbBO_3$ with these two different connection styles. We find that the hybridization between the Pb *p* orbitals and the BO_3 π orbitals is *larger* in the $PbBO_3$ structure with the *closed* Pb−B−O ring (Figure 1a), while more localized atomic-like Pb *p* orbitals and BO_3 π orbitals are found in the *open* Pb−B−O connection (Figure 1b). An open lead−oxygen connection will then result in lead−oxygen bonds that are less responsive to optical excitation; the polarizability of the chemical bond contributes less to the SHG response, which in the compound would largely originates in polar (static) atomic distortions. In $Pb_2B_5O_9Cl$, the linkage between BO_4 and BO_3 groups makes it much easier to form the open Pb−O−B ring than a closed Pb−O−B−O quadrangle ring connection. This unique open connection and strong localization of orbitals make the Pb−O bonds less polarizable, resulting in a small SHG response.[35]

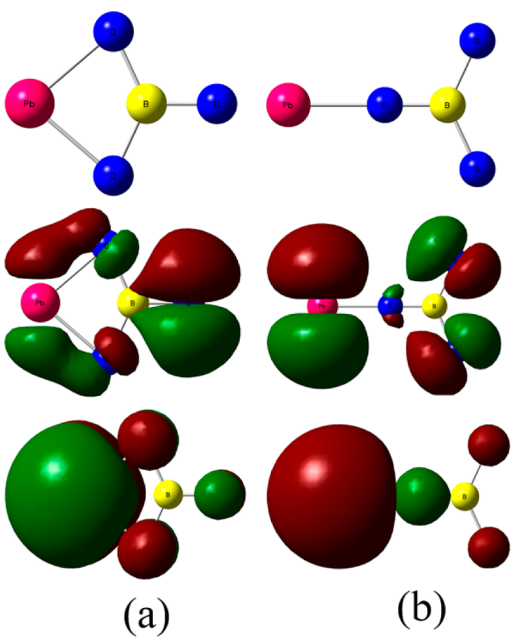

Figure 1. Diagram of the structures and the frontier molecular orbitals (isovalue 0.02 au/Å^3) of $PbBO_3$ with (a) closed (left) or (b) open (right) Pb−B−O ring configuration. The $PbBO_3$ clusters are shown in the top panels. The HOMO and LUMO are shown in the middle and lower panels, respectively. The pink, yellow, and blue spheres represent the lead, boron, and oxygen atoms.

Closed Pb−B−O rings are more easily obtained in compounds with isolated BO_3 groups. Owing to both chelation between the oxygen atoms and the Pb(II) cation and the SCALP Pb(II), A-L replacement has the capability to improve the SHG response provided that the optimal anion environment is realized. To investigate the viability of enhancing SHG with this type of A-L replacement, we designed and synthesized a novel lead borate, $Pb_2Ba_3(BO_3)_3Cl$, with the desired Pb−O chelation. It exhibits an SHG efficiency that is 3.2 × KDP and 6 times larger than that of isomorphic $Ba_5(BO_3)_3Cl$. To the best of our knowledge, $Pb_2Ba_3(BO_3)_3Cl$ is the first acentric lead barium borate with an isolated BO_3 group. The observed SHG enhancement is a direct result of the closed ring geometry, and this understanding provides a reliable guideline for selecting borate structures for A-L replacement.

RESULTS

Crystal Growth of $Pb_2Ba_3(BO_3)_3Cl$. The crystals of $Pb_2Ba_3(BO_3)_3Cl$ were grown by the spontaneous crystallization method. Sintered powders of $Pb_2Ba_3(BO_3)_3Cl$ were placed in a platinum crucible, which was put in a programmable temperature controlled growth furnace. The growth furnace was quickly heated to 780 °C and held at that temperature for 48 h. The furnace was then cooled to 730 °C at a rate of 1 °C/h and then cooled to room temperature at a rate of 10 °C/h, resulting in $Pb_2Ba_3(BO_3)_3Cl$ crystals. Additional details are given in the Methods section.

Structure Comparison. $Pb_2Ba_3(BO_3)_3Cl$ crystallizes in the chiral orthorhombic space group $C222_1$ (no. 20) with lattice parameters a = 10.4706(11) Å, b = 14.4379(15) Å, c = 7.9454(9) Å, Z = 4. There is one unique Pb atom in general position (8*c*), three unique Ba atoms (4*a*, 4*b* and 4*b*), two unique B atoms (4*a* and 8*c*), five unique O atoms (8*c*, 8*c*, 4*a*, 8*c*, and 8*c*), and one unique Cl atom (4*b*). More details about the crystal data and structure refinement are shown in Table S1 in the Supporting Information (SI). The structure of $Pb_2Ba_3(BO_3)_3Cl$ consists of two types of isolated BO_3 units alternatively arranged in pseudolayers along the *b* axis, with Ba^{2+} and Pb^{2+} cations filling the gaps (Figure 2). The $B(1)O_3$ group is oriented perpendicular to the *b* axis while the $B(2)O_3$ group is tilted. The presence of these isolated BO_3 groups was further confirmed by IR spectroscopy (Figure S1, SI). The Pb^{2+} cations are surrounded by six O atoms, forming a distorted polyhedra, which share an edge with the $B(1)O_3$ group, resulting in a closed Pb−O−B−O quadrangle (Figure 2, right).

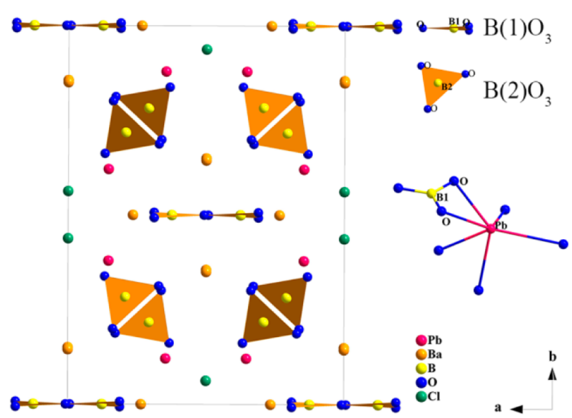

Figure 2. Crystal structure of $Pb_2Ba_3(BO_3)_3Cl$ (left panel) and a closed Pb−O−B−O ring (right panel).

It is meaningful to make comparisons between $Pb_2Ba_3(BO_3)_3Cl$ and its isomorph $Ba_5(BO_3)_3Cl$.[36] $Ba_5(BO_3)_3Cl$ crystallizes in the same $C222_1$ space group (no. 20) with similar lattice parameters: a = 10.4549(5) Å, b = 14.8789(8) Å, c = 7.8701(4) Å, Z = 4. Like $Pb_2Ba_3(BO_3)_3Cl$, there are two unique B atoms (4*a* and 8*c*), five unique O atoms (8*c*, 8*c*, 4*a*, 8*c*, and

DOI: 10.1021/jacs.5b05406
J. Am. Chem. Soc. 2015, 137, 9417−9422

8c), and one unique Cl atom (4b); however, there are four unique Ba atoms (4a, 4b, 4b, and 8c). $Pb_2Ba_3(BO_3)_3Cl$ is therefore obtained by replacement of Ba atoms at the 8c crystallographic sites in $Ba_5(BO_3)_3Cl$ with Pb atoms. In this structure, two oxygen atoms are bonded to Pb in a closed ring connection. This substitution results in a shrinking of the *b* axis and elongation of the *c* axis; this may be caused by the lone pair electrons of the Pb atoms causing a distortion of the polyhedra.

UV−vis−NIR Diffuse Reflectance Spectra and Powder SHG Measurement. The UV−vis−NIR diffuse reflectance spectra for $Pb_2Ba_3(BO_3)_3Cl$ were recorded at room temperature with a SolidSpec-3700 DUV spectrophotometer using fluororesin as a standard in the wavelength range from 300 to 2600 nm (Figure 3a). Reflectance spectra were converted to absorbance using the Kubelka−Munk function.[41,42] As shown in Figure 3a, the absorption edge is located at 312 nm (the optical band gap is therefore 3.97 eV).

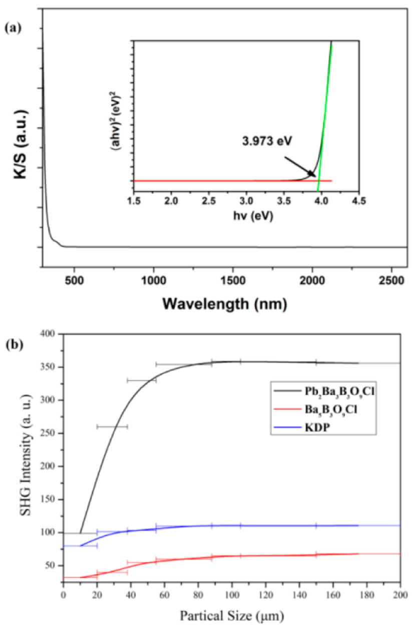

Figure 3. (a) UV−vis−NIR diffuse spectrum of $Pb_2Ba_3(BO_3)_3Cl$. (b) Phase-matching curves of $Pb_2Ba_3(BO_3)_3Cl$, $Ba_5(BO_3)_3Cl$, and KDP. The solid curve drawn is to guide the eye and is not a fit to the data.

The SHG response was measured on powdered samples by the Kurtz and Perry method with a 1064 nm Q-switched laser.[43] The plots of the SHG signals as a function of particle size measured on ground samples suggest phase-matching behavior at 1064 nm. The SHG intensity for $Pb_2Ba_3(BO_3)_3Cl$ is about 3.2 times that of KDP for particle sizes of 88−105 μm. In order to compare the SHG response of $Pb_2Ba_3(BO_3)_3Cl$ with $Ba_5(BO_3)_3Cl$, a sample of $Ba_5(BO_3)_3Cl$ was prepared by a high temperature solid reaction. The SHG effect of $Pb_2Ba_3(BO_3)_3Cl$ is about 6 times that of $Ba_5(BO_3)_3Cl$ (Figure 3b).

■ DISCUSSION

The primary question arising from these results is where does the SHG enhancement originate after this A-L replacement? To address this, we investigated the electronic and optical properties of $Pb_2Ba_3(BO_3)_3Cl$ and isomorphic $Ba_5(BO_3)_3Cl$ using first-principles density functional theory (DFT) calculations (see Methods for calculation details). As can be seen from the atom- and orbital-resolved electronic density of states (DOS) for $Pb_2Ba_3(BO_3)_3Cl$ (Figure 4), the energy window from −5 to 0 eV primarily consists of O 2*p* states, Cl 3*p* states,

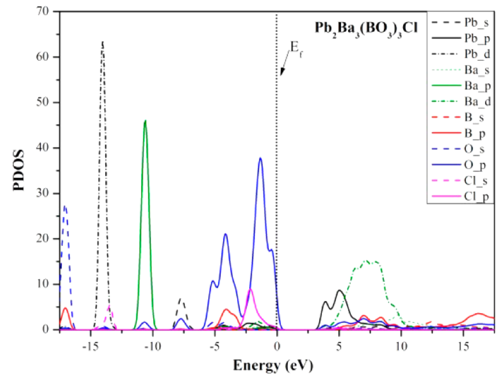

Figure 4. Projected density of states (PDOS) of $Pb_2Ba_3(BO_3)_3Cl$.

B 2*sp* mixed states, and Pb 6*sp* mixed states. However, the top of the valence band consists almost exclusively of O 2*p* states, while the bottom of the conduction band is primarily Pb *sp* states, with small contributions from the Ba *d*, O 2*p*, Cl *p*, and B *sp* states. The electronic structure around the band edges is thus mainly derived from the PbO and BO_3 groups, which provide the dominant states in the optical matrix elements describing the virtual excitations responsible for the NLO effect in $Pb_2Ba_3(BO_3)_3Cl$.

The formation of distorted PbO polyhedra arises from the asymmetric lone pair electron density derived from the interaction of the Pb cation *p* states with the cation *s*-oxygen *p* antibonding orbitals[44,45] (Figure 4). The Pb *s*-O *p* overlap can be seen at −7.5 eV, a feature which is missing from the PDOS of $Ba_5(BO_3)_3Cl$ (Figure S3 in the SI). The covalent interactions between the Pb and O states of the chelated BO_3 unit result in shorter Pb−O bonds and a shift of the O 2*p* states to lower energy. Another important consequence of Pb substitution for Ba is that the 6*p* states of Pb are closer in energy with the Cl *p* states. The Pb 6*p*−Cl 3*p* π-interactions and hybridization lead to dispersive Cl states from −2.5 eV to the valence band edge, i.e., over the same energy range from which the O 2*p* spectral weight transfer occurs. In $Ba_5(BO_3)_3Cl$ this interaction cannot occur and thus the Cl 3*p* states are localized (centered about −2.5 eV, Figure S3 in the SI). The Pb states and the change in Pb−O covalency in $Pb_2Ba_3(BO_3)_3Cl$ also result in the band gap reduction compared to $Ba_5(BO_3)_3Cl$. The redistribution of these electronic states, mediated by Pb substitution and the distorted lead−oxygen polyhedra, enhances the SHG response.

It is well-known that the SHG response of a crystal is determined by the cooperation of the intrinsic dipole moment and induced dipole oscillations.[46] The structure of $Pb_2Ba_3(BO_3)_3Cl$ is chiral and, therefore, does not have a unique anisotropic axis; because of this, the induced dipole moment resulting from the flexibility of the electronic density involved in various chemical bonds plays an important role in determining the SHG response.[47] Generally speaking, the more flexible the chemical bonds in the basic units, the larger the SHG response in the crystal. The flexibility of the electronic motion in a chemical bond is inversely proportional to its degree of covalent character; that is, a more covalent bond will have a greater amount of electronic charge along the bond, granting less flexibility. Using a quantitative metric based on the degree of overlap between the atomic orbitals forming the

DOI: 10.1021/jacs.5b05406
J. Am. Chem. Soc. 2015, 137, 9417−9422

bond,[48] we computed the covalency of the Pb−O or Ba−O bonds in these materials (Figure 5). Note that on this scale a value of C_{M-O} closer to zero indicates a more covalent bond between the metal cation and oxygen.

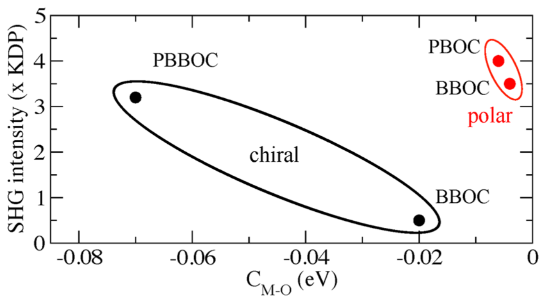

Figure 5. Covalency of the M−O (M = Pb or Ba) bonds (C_{M-O})in chiral *C*222$_1$ $Pb_2Ba_3(BO_3)_3Cl$ (PBBOC) and $Ba_5(BO_3)_3Cl$ (BBOC) and polar *Pnn*2 $Pb_2B_5O_9Cl$ (PBOC) and $Ba_2B_5O_9Cl$ (BBOC). The M−O covalency in PBBOC is given as a weighted average of the Pb and Ba bonds.

The M−O bonds in chiral $Ba_5(BO_3)_3Cl$ are very covalent, while substitution of the more electronegative Pb (to create $Pb_2Ba_3(BO_3)_3Cl$) significantly decreases this covalency. Because a less covalent bond will be more polarizable under optical excitation, replacing Ba with Pb results in an enhancement of SHG response: It decreases the average covalency of the M−O bonds while producing an asymmetric and somewhat delocalized charge density owing to the chelation (see the middle panels of Figure 1). While the same effect can be seen in the polar isomorphs $Pb_2B_5O_9Cl$ and $Ba_2B_5O_9Cl$, the change in the SHG response is much smaller due to the difference in how the electronic charge is distributed in a polar or chiral compound. Because of the cooperative polar displacements, the structural contribution to the SHG response dominates in polar compounds;[23,49] in a chiral compound, which does not have these displacements, the electronic contribution (as quantified by the bond covalency metric in Figure 5) takes on much more importance.

In summary, motivated by the large SHG response obtained from combinations of diverse types of active NLO groups, and the properties of isolated boron−oxygen groups and lead−oxygen groups, we synthesized and characterized the acentric compound $Pb_2Ba_3(BO_3)_3Cl$ with isolated BO_3 groups. The phase-matching SHG response of $Pb_2Ba_3(BO_3)_3Cl$ is about 3.2 times that of KDP, and as large as 6 times that of isomorphic $Ba_5(BO_3)_3Cl$. After examining the relationship between the SHG response and the electronic structure, we find that the enhanced response originates from the unique edge sharing connection style between the Pb−O polyhedra and B−O groups. The unique connection style makes the metal−oxygen bond more polarizable to external optical excitation. Hence, we conjecture that among lead A-L replacement borates, those compounds with isolated boron−oxygen building units would be potential NLO materials with enhanced SHG responses and merit continued investigation.

■ METHODS

Synthesis of $Pb_2Ba_3(BO_3)_3Cl$. Polycrystalline samples of $Pb_2Ba_3(BO_3)_3Cl$ were prepared by the standard solid-state reaction. The stoichiometric mixtures of PbO (Beijing Huagong Chemical Co., Ltd., 99.9%), $Ba(NO_3)_2$ (Shenyang Xinxi Chemical Co., Ltd., 99.5%), $BaCl_2$ (Shenyang Xinxi Chemical Co., Ltd., 99.5%), and H_3BO_3 (Tianjin Baishi Chemical Co., Ltd., 99.5%) were completely ground in an agate mortar and then calcined at 300 °C for 12 h and then 500 °C for 5 h in a muffle furnace. The mixture was cooled to room temperature, finely ground again, then heated to 715 °C, and held at this temperature for 48 h until the pure powders of the title compounds were obtained. The phase purity was confirmed by powder X-ray diffraction (XRD), and the XRD pattern matches the one calculated from single-crystal XRD analysis very well (see Figure S2 in the SI). Single crystals of the title compounds were grown by the spontaneous crystallization method. The sintered powders of $Pb_2Ba_3(BO_3)_3Cl$ were placed in a platinum crucible, which was put in a programmable temperature controlled growth furnace. The growth furnace was quickly heated to 780 °C followed by dwelling at that temperature for 48 h. The furnace was cooled to 730 °C at a rate of 1 °C/h and then cooled to room temperature at a rate of 10 °C/h. As a result, the $Pb_2Ba_3(BO_3)_3Cl$ crystals were obtained.

Physical Property Measurements. The powder XRD data were collected at room temperature in the angular range of 2θ = 10°−70° with a scan step width of 0.02° and a fixed counting time of 1 s/step using an automated Bruker D2 X-ray diffractometer with Cu Kα radiation (λ = 1.5418 Å). A transparent, block crystal of $Pb_2Ba_3(BO_3)_3Cl$ with sizes of 0.12 mm × 0.08 mm × 0.08 mm was mounted on a glass fiber for a single-crystal X-ray determination study. The diffraction data were collected at room temperature on a Bruker Smart APEX II single crystal diffratometer equipped with a CCD-detector (Mo K$_\alpha$ radiation, λ = 0.71073 Å). The reduction of data were carried out with the Bruker Suite software package.[50] A multiscan absorption correction was performed with the SADABS program.[51] The structure was solved by direct methods and refined by the full-matrix least-squares method in the SHELXL-97 system.[52] The structure was checked for missing symmetry elements with PLATON.[53] All atoms were refined with anisotropic displacement parameters. Details of crystal parameters, data collection, and structure refinement are listed in Table S1 in the SI. Final atom coordinates and equivalent isotropic displacement parameters are listed in Table S2 in the SI. Selected bond distances and angles are given in Table S1 in the SI.

The SHG responses were measured on powdered samples by the Kurtz and Perry method with a 1064 nm Q-switch laser. All of the samples were ground and sieved into a series of distinct particle size ranges of <20, 20−38, 38−55, 55−88, 88−105, 105−150, and 150−200 μm, respectively, which were pressed into a disk with diameter of 3 mm that was put between glass microscope slides and secured with tape in a 1 mm thick aluminum holder, and the powdered KDP sample was used as the reference.

Computational Methods. To better understand the origin of the enhanced SHG response, the electronic structure and the optical properties of a series of borates were calculated using density functional theory[54,55] as implemented in the CASTEP package[56] with the generalized gradient approximation (GGA) with the Perdew−Burke−Ernzerhof (PBE) functional.[57,58] During the calculations, the structures were fixed to the experimental crystallographic data determined by single crystal XRD. Norm-conserving pseudopotentials were used with the following valence electron configurations: Pb-$5s^25p^65d^{10}6s^26p^2$, Ba-$5s^25p^66s^2$, B-$2s^22p^1$, O-$2s^22p^4$, and Cl-$3s^23p^5$. The number of

DOI: 10.1021/jacs.5b05406
J. Am. Chem. Soc. 2015, 137, 9417−9422

plane waves included in the basis was determined by a cutoff energy of 830 eV (for $Ba_5(BO_3)_3Cl$), 910 eV (for $Pb_2Ba_3(BO_3)_3Cl$). The numerical integration of the Brillouin zone was performed using a 3 × 3 × 3 ($Ba_5(BO_3)_3Cl$, and $Pb_2Ba_3(BO_3)_3Cl$) Monkhorst−Pack *k*-point sampling.[59] The other calculation parameters and convergent criteria were the default values of the CASTEP code.

For calculation of the bond covalency, we performed DFT calculations as implemented in the Vienna *Ab initio* Software Package (VASP),[60,61] with GGA-PBE, a 600 eV plane-wave cutoff, and the projector augmented-wave (PAW) potentials[62] with a $5d^{10}6s^26p^2$ valence electron configuration for Pb, $5s^25p^66s^2$ for Ba, $2s^22p^1$ for B, $2s^22p^4$ for O, and $3s^23p^5$ for Cl. An 11 × 9 × 9 and 7 × 9 × 11 Monkhorst−Pack *k*-point mesh was used for the chiral and polar compounds, respectively, in each case.

The molecular orbitals of the $PbBO_3$ units were calculated using the DFT within the B3LYP/LanL2DZ level as implemented in Gaussian09 code[63] following the prescription given in ref 22.

■ ASSOCIATED CONTENT

Supporting Information

Crystal data and structure refinement; atomic coordinates and equivalent isotropic displacement parameters; selected bond lengths and angles; IR spectrum; the powder X-ray diffraction pattern and the calculated pattern based on the single crystal data of $Pb_2Ba_3(BO_3)_3Cl$. The projected density of states (PDOS) of $Ba_5(BO_3)_3Cl$. The Supporting Information is available free of charge on the ACS Publications website at DOI: 10.1021/jacs.5b05406.

■ AUTHOR INFORMATION

Corresponding Authors

*zhyang@ms.xjb.ac.cn (Z.Y.)
*slpan@ms.xjb.ac.cn (S.P.)
*jrondinelli@northwestern.edu (J.R.)

Author Contributions

#X.D. and Q.J. contributed equally.

Notes

The authors declare no competing financial interest.

■ ACKNOWLEDGMENTS

This work is supported by the National Basic Research Program of China (Grant No. 2014CB648400), National Natural Science Foundation of China (Grant Nos. 51425206, U1129301, 11104344, 51172277), "Western Light Joint Scholar Foundation" Program of CAS (Grant No. LHXZ201101), the Recruitment Program of Global Experts (1000 Talent Plan, Xinjiang Special Program), Xinjiang International Science & Technology Cooperation Program (20146001), and the Funds for Creative Cross & Cooperation Teams of CAS. K.R.P. acknowledges support from the National Science Foundation (Solid State Chemistry Award No. DMR-1307698); J.Y. and J.M.R. acknowledge support from NSF CAREER Award No. DMR-145688.

■ REFERENCES

(1) Becker, P. *Adv. Mater.* **1998**, *10*, 979.
(2) Chung, I.; Kanatzidis, M. G. *Chem. Mater.* **2014**, *26*, 849.
(3) Yao, W. J.; He, R.; Wang, X. Y.; Lin, Z. S.; Chen, C. T. *Adv. Opt. Mater.* **2014**, *2*, 411.
(4) Xia, Y. N.; Chen, C. T.; Tang, D. Y.; Wu, B. C. *Adv. Mater.* **1995**, *7*, 79.
(5) Chen, C. T.; Wang, Y. B.; Wu, B. C.; Wu, K. C.; Zeng, W. L.; Yu, L. H. *Nature* **1995**, *373*, 322.
(6) Yu, P.; Wu, L. M.; Zhou, L. J.; Chen, L. *J. Am. Chem. Soc.* **2014**, *136*, 480.
(7) Wu, H. P.; Yu, H. W.; Pan, S. L.; Huang, Z. J.; Yang, Z. H.; Su, X.; Poeppelmeier, K. R. *Angew. Chem. Int. Ed.* **2013**, *52*, 3406.
(8) Chen, M. C.; Wu, L. M.; Lin, H.; Zhou, L. J.; Chen, L. *J. Am. Chem. Soc.* **2012**, *134*, 6058.
(9) Yu, P.; Zhou, L. J.; Chen, L. *J. Am. Chem. Soc.* **2012**, *134*, 2227.
(10) Lin, H.; Chen, L.; Zhou, L. J.; Wu, L. M. *J. Am. Chem. Soc.* **2013**, *135*, 12914.
(11) Chen, C. T.; Wu, B. C.; Jiang, A. D.; You, G. M. *Sci. Sin. B* **1985**, *28*, 235.
(12) Chen, C. T.; Wu, Y. C.; Jiang, A. D.; Wu, B. C.; You, G. M.; Li, R. K.; Lin, S. J. *J. Opt. Soc. Am. B* **1989**, *6*, 616.
(13) Wu, Y. C.; Sasaki, T.; Nakai, S.; Yokotani, A.; Tang, H. G.; Chen, C. T. *Appl. Phys. Lett.* **1993**, *62*, 2614.
(14) Mori, Y.; Kuroda, I.; Nakajima, S.; Sasaki, T.; Nakai, S. *Appl. Phys. Lett.* **1995**, *67*, 1818.
(15) Wu, B. C.; Tang, D. Y.; Ye, N.; Chen, C. T. *Opt. Mater.* **1996**, *5*, 105.
(16) Boyd, G. D.; Kasper, H.; McFee, J. H. *IEEE J. Quantum Electron.* **1971**, *7*, 563.
(17) Tell, B.; Kasper, H. M. *Phys. Rev. B* **1971**, *4*, 4455.
(18) Harasaki, A.; Kato, K. *Jpn. J. Appl. Phys.* **1997**, *36*, 700.
(19) Boyd, G. D. *Appl. Phys. Lett.* **1971**, *18*, 301.
(20) Zou, G. H.; Ye, N.; Huang, L.; Lin, X. S. *J. Am. Chem. Soc.* **2011**, *133*, 20001.
(21) Kang, L.; Lin, Z. S.; Qin, J. G.; Chen, C. T. *Sci. Rep.* **2013**, *3*, 1366.
(22) Zou, G. H.; Huang, L.; Ye, N.; Lin, C. S.; Cheng, W. D.; Huang, H. *J. Am. Chem. Soc.* **2013**, *135*, 18560.
(23) Tran, T. T.; Halasyamani, P. S.; Rondinelli, J. M. *Inorg. Chem.* **2014**, *53*, 6241.
(24) Bera, T. K.; Song, J. H.; Freeman, A. J.; Jang, J. I.; Ketterson, J. B.; Kanatzidis, M. G. *Angew. Chem. Int. Ed.* **2008**, *47*, 7828.
(25) Bera, T. K.; Jang, J. I.; Ketterson, J. B.; Kanatzidis, M. G. *J. Am. Chem. Soc.* **2009**, *131*, 75.
(26) Ra, H. S.; Ok, K. M.; Halasyamani, P. S. *J. Am. Chem. Soc.* **2003**, *125*, 7764.
(27) Shi, Y. J.; Pan, S. L.; Dong, X. Y.; Wang, Y.; Zhang, M.; Zhang, F. F.; Zhou, Z. X. *Inorg. Chem.* **2012**, *51*, 10870.
(28) Pan, S. L.; Smit, J. P.; Marvel, M. R.; Stampler, E. S.; Haag, J. M.; Baek, J.; Halasyamani, P. S.; Poeppelmeier, K. R. *J. Solid State Chem.* **2008**, *181*, 2087.
(29) Belik, A. A.; Rusakov, D. A.; Furubayashi, T.; Takayama-Muromachi, E. *Chem. Mater.* **2012**, *24*, 3056.
(30) Halasyamani, P. S.; Poeppelmeier, K. R. *Chem. Mater.* **1998**, *10*, 2753.
(31) Halasyamani, P. S. *Chem. Mater.* **2004**, *16*, 3586.
(32) Zhang, W. L.; Cheng, W. D.; Zhang, H.; Geng, L.; Lin, C. S.; He, Z. Z. *J. Am. Chem. Soc.* **2010**, *132*, 1508.
(33) Belokoneva, E. L.; Kabalov, Y. K.; Dimitrova, O. V.; Stefanovich, S. Y. *Crystallogr. Rep.* **2003**, *48*, 44.
(34) Huang, Y. Z.; Wu, L. M.; Wu, X. T.; Li, L. H.; Chen, L.; Zhang, Y. F. *J. Am. Chem. Soc.* **2010**, *132*, 12788.
(35) Chen, Z. H.; Pan, S. L.; Yang, Z. H.; Dong, X. Y.; Su, X.; Yang, Y. *J. Mater. Sci.* **2013**, *48*, 2590.
(36) Chen, Z. H.; Pan, S. L.; Zhao, W. W.; Yang, Y.; Wu, H. P.; Zhang, F. F. *J. Synth. Cryst.* **2011**, *40*, 1394.
(37) Yu, H. W.; Wu, H. P.; Pan, S. L.; Yang, Z. H.; Su, X.; Zhang, F. F. *J. Mater. Chem.* **2012**, *22*, 9665.
(38) Huang, Z. J.; Su, X.; Pan, S. L.; Dong, X. Y.; Han, S. J.; Yu, H. W.; Zhang, M.; Yang, Y.; Cui, S. F.; Yang, Z. H. *Scr. Mater.* **2013**, *69*, 449.
(39) Li, H. Y.; Wu, H. P.; Su, X.; Yu, H. W.; Pan, S. L.; Yang, Z. H.; Lu, Y.; Han, J.; Poeppelmeier, K. R. *J. Mater. Chem. C* **2014**, *2*, 1704.

(40) Burns, P. C.; Grice, J. D.; Hawthorne, F. C. *Can. Mineral.* **1995**, *33*, 1131.
(41) Kubelka, P.; Munk, F. Z. *Technol. Phys.* **1931**, *12*, 593.
(42) Tauc, J. *Mater. Res. Bull.* **1970**, *5*, 721.
(43) Kurtz, S. K.; Perry, T. T. *J. Appl. Phys.* **1968**, *39*, 3798.
(44) Walsh, A.; Payne, D. J.; Egdell, R. G.; Watson, G. W. *Chem. Soc. Rev.* **2011**, *40*, 4455.
(45) Payne, D. J.; Egdell, R. G.; Walsh, A.; Watson, G. W.; Guo, J.; Glans, P. A.; Learmonth, T.; Smith, K. E. *Phys. Rev. Lett.* **2006**, *96*, 157403.
(46) Jiang, X.; Zhao, S.; Lin, Z.; Luo, J.; Bristowe, P. D.; Guan, X.; Chen, C. *J. Mater. Chem. C* **2014**, *2*, 530.
(47) Cammarata, A.; Zhang, W. G.; Halasyamani, P. S.; Rondinelli, J. M. *Chem. Mater.* **2014**, *26*, 5773.
(48) Cammarata, A.; Rondinelli, J. M. *J. Chem. Phys.* **2014**, *141*, 114704.
(49) Cammarata, A.; Rondinelli, J. M. *ACS Photonics* **2014**, *1*, 96.
(50) *Bruker Suite, v.*Bruker AXS Inc.: Madison, WI, USA, 2008.
(51) *Bruker SMART, V., and SADABS, version 2.05*; Bruker Analytical X-ray Systems, Inc.: Madison, WI, 2003.
(52) Sheldrick, G. M. *SHELXTL-97 Sheldrick: Program for Crystal Structure Refinement*; University of Göttingen: Germany,1997.
(53) Spek, A. L. *J. Appl. Crystallogr.* **2003**, *36*, 7.
(54) Hohenberg, P.; Kohn, W. *Phys. Rev.* **1964**, *136*, B864.
(55) Kohn, W.; Sham, L. J. *Phys. Rev.* **1965**, *140*, A1133.
(56) Clark, S. J.; Segall, M. D.; Pickard, C. J.; Hasnip, P. J.; Probert, M. J.; Refson, K.; Payne, M. C. *Z. Kristallogr.* **2005**, *220*, 567.
(57) Perdew, J. P.; Jackson, K. A.; Pederson, M. R.; Singh, D. J.; Fiolhais, C. *Phys. Rev. B: Condens. Matter Mater. Phys.* **1992**, *46*, 6671.
(58) Perdew, J. P.; Burke, K.; Ernzerhof, M. *Phys. Rev. Lett.* **1996**, *77*, 3865.
(59) Monkhorst, H. J.; Pack, J. D. *Phys. Rev. B* **1976**, *13*, 5188.
(60) Kresse, G.; Furthmüller, J. *Comput. Mater. Sci.* **1996**, *6*, 15.
(61) Kresse, G.; Hafner, J. *Phys. Rev. B: Condens. Matter Mater. Phys.* **1993**, *47*, 558.
(62) Blöchl, P. E. *Phys. Rev. B: Condens. Matter Mater. Phys.* **1994**, *50*, 17953.
(63) Frisch, M. J.; Trucks, G. W.; Schlegel, H. B.; Scuseria, G. E.; Robb, M. A.; Cheeseman, J. R.; Scalmani, G.; Barone, V.; Mennucci, B.; Petersson, G. A.; Nakatsuji, H.; Caricato, M.; Li, X.; Hratchian, H. P.; Izmaylov, A. F.; Bloino, J.; Zheng, G.; Sonnenberg, J. L.; Hada, M.; Ehara, M.; Toyota, K.; Fukuda, R.; Hasegawa, J.; Ishida, M.; Nakajima, T.; Honda, Y.; Kitao, O.; Nakai, H.; Vreven, T.; Montgomery, J. A., Jr.; Peralta, J. E.; Ogliaro, F.; Bearpark, M.; Heyd, J. J.; Brothers, E.; Kudin, K. N.; Staroverov, V. N.; Kobayashi, R.; Normand, J.; Raghavachari, K.; Rendell, A.; Burant, J. C.; Iyengar, S. S.; Tomasi, J.; Cossi, M.; Rega, N.; Millam, J. M.; Klene, M.; Knox, J. E.; Cross, J. B.; Bakken, V.; Adamo, C.; Jaramillo, J.; Gomperts, R.; Stratmann, R. E.; Yazyev, O.; Austin, A. J.; Cammi, R.; Pomelli, C.; Ochterski, J. W.; Martin, R. L.; Morokuma, K.; Zakrzewski, V. G.; Voth, G. A.; Salvador, P.; Dannenberg, J. J.; Dapprich, S.; Daniels, A. D.; Farkas, Ö.; Foresman, J. B.; Ortiz, J. V.; Cioslowski, J.; Fox, D. J. *Gaussian 09*, Revision D.01; Gaussian Inc.: Wallingford, CT, 2009.

DOI: 10.1021/jacs.5b05406
J. Am. Chem. Soc. 2015, 137, 9417−9422